Journal of Alloys and Compounds, 197 (1993) 271–280
JALCOM 7306

Local atomic environments of hard magnets, metallic glasses, and icosahedral phases

L. H. Bennett
National Institute of Standards and Technology, Gaithersburg, MD 20899 (USA)

R. E. Watson
Brookhaven National Laboratory, Upton, NY 11973 (USA)

Abstract

Voronoi polyhedra furnish a useful measure of the local environment of an atom, including a description of the site symmetry of the atom, and a catalog of what atoms constitute its nearest neighbors. A modified Voronoi construction also accounts for the relative sizes of the various atoms. Several applications of such polyhedra are presented, including magnetic moments and anisotropies in hard magnets, polymorphism in metallic glasses, local environments in quasicrystals, and supersymmetry in αMn.

1. Introduction

One useful measure of the local environment of an atom is the Voronoi (also known as Wigner–Seitz or Dirichlet) polyhedron construction. Such polyhedra provide useful insight into the understanding of various properties, including magnetic coupling or chemical bonding, as reflected in the local environment. Some of the attributes of local environment determined from the Voronoi polyhedron are (i) from the number of faces in the polyhedron, the coordination number and an identification of those atoms which constitute the nearest neighbors to the site in question, (ii) from the number of edges in a face, the number of nearest neighbors common to a near-neighbor pair, (iii) the local site symmetry arising from the presence of these neighbors, and (iv) the volume of the atom. Such attributes can be of interest in and of themselves for some given crystalline phase and, more importantly, they can also be relevant to comparisons of one crystal structure with another as they affect some properties.

The traditional method for constructing Voronoi polyhedra is to draw perpendicular bisecting planes across the lines connecting the atom in question to the atoms in its vicinity. Such a scheme fails to account for the relative sizes of the different atomic species and fails to pick up polyhedra faces if they do not intersect the bond line between the two atoms in question. (Such facets do occasionally occur.) A procedure, known as the "radical construct" [1] positions the bounding planes in proportion to assigned atomic radii of the atoms, while maintaining the essential space-filling nature of the resulting set of Voronoi polyhedra.

The volumes of the individual Voronoi polyhedra and the areas of individual polyhedron facets depend, of course, on the relative magnitudes of the radii attributed to the different atomic sites. Sometimes the topology of a polyhedron (*i.e.* the number of facets, the juxtaposition of each facet with respect to the others, and the number of edges for each facet) remains unchanged as a function of varying the relative magnitudes of the radii. This topological stability is the circumstance for chemically reasonable variations in the elemental radii for many systems, including the Frank–Kasper phases to be discussed below. For some systems, particularly the transition-metal–metalloid systems discussed in Section 4, the topologies of the resulting Voronoi polyhedra depend sensitively on the choice of radii used in their construction and where widely varying "reasonable" choices of radii may be made.

It is common to catalog a Voronoi polyhedra by enumerating how many facets, having some given number of edges, occur, *i.e.* (a, b, c, d, ...) denotes a polyhedron having a triangular facets, b four-sided facets, c five-sided facets, etc. The number of edges on a facet indicates how many nearest neighbors are common to the nearest-neighbor pair responsible for the facet. Any number of zeros can be added to the designation. (Often the designation (a, b, c, d, ...) completely defines the topology of the Voronoi polyhedron. However, there are situations where more than

0925-8388/93/$6.00

one geometric arrangement of a given set of facets can be made and then the designation is, of course, incomplete. This issue is not a concern in the present paper.)

What is the chemical information indicated in a Voronoi polyhedron construction? First, it is reasonable to assume that those neighbors contributing facets to the polyhedra of an atom are the neighbors which may be important to the bonding of that atom. In addition, the relative areas of a pair of facets provide a crude measure of the relative importance of the bonding associated with the neighboring atoms contributing to those facets. Finally, consider two bond lines, one having n common nearest neighbors (implying n edges to the facet) along the bond line while the other has greater than n common neighbors. The latter, having more such neighbors, will tend to have these neighbors spread out further radially from the bond line and this will tend to allow the closer approach of the two atoms on the bond line. Having more common nearest neighbors and having closer approach, the latter bond will thus tend to be more important chemically (and magnetically). Therefore, all other things being equal, Voronoi polyhedra facets having larger numbers of edges can be expected to play the larger role in bonding. This is certainly the case for the so-called topologically close-packed or Frank–Kasper phases of which more will be said shortly.

The Voronoi polyhedra for several basic crystal structures are tabulated in Table 1. A few of these are illustrated in Fig. 1. The numbers of "near neighbors", as measured by the numbers of facets, are in agreement with the usual definition of atomic coordination for these systems. For example, the f.c.c. structure, designated (0, 12) or (0, 12, 0), is, as usual, 12-fold coordinated. However, the b.c.c. structure, as defined by the Voronoi construction (0, 6, 0, 8), is 14-fold coordinated, having six "second-nearest neighbors" (represented by the four-sided facets of the Voronoi polyhedron, as well as eight slightly closer "nearest neighbors" (with the larger six-sided facets). Also shown in Fig. 1 are the 16-fold coordinated sites found especially in Frank–Kasper phases, and the nine-fold coordinated Bernal environment important in glass formation. Values of q, the average number of edges on a facet, are also listed in Table 1. This quantity provides one meaningful measure of the packing in a structure. The b.c.c.-, h.c.p.- and f.c.c.-based phases have Voronoi polyhedra made up predominantly of four- and six-edged facets. This contrasts with the Frank–Kasper phases which have largely five-edged facets with small numbers of six-edged ones.

The Frank–Kasper phases [2] involve atoms packed in 12-, 14-, 15-, and 16-fold environments. Twelve of the nearest neighbors share five common nearest neighbors along the bond line to the central atom. In addition, the 14-, 15-, and 16-fold environments involve, respectively, two, three, and four nearest neighbors which share six commonnearest neighbors with the center atoms. Having six, as compared with five, common neighbors will generally imply that these common neighbors lie further out radially from the bond line, thus allowing the two atoms on the bond line to be closer together. The closer proximity, and the sharing of more common nearest neighbors, both should affect the chemical and magnetic coupling along these bond lines.

TABLE 1. Voronoi polyhedra for several basic prototype structures. $\langle q \rangle$ is the average number of edges on a facet

Structure type	Atom	Polyhedron	Total coordination	Constraint on radii	$\langle q \rangle$
Simple cubic	All	0 6	6	–	4.0
B.c.c. (and CsCl)	All	0 6 0 8	14	–	5.14286...
H.c.p.	All	0 12	12	–	4.0
F.c.c	All	0 12	12	–	4.0
Cu_3Au (Y_3X)	X at corner	0 12	12	$R_X < R_Y$	4.5
	Y at face center	0 4 8	12		
Cu_3Au (Y_3X)	X at corner	0 6 0 12	18	$R_X > R_Y$	4.8339...
	Y at face center	0 8 0 4	12		
NaCl	X or Y	0 6	6	$R_X = R_Y$	4.0
NaCl	X	0 6	6	$R_X < R_Y$	5.0
	Y	0 6 0 12	18		
9-fold Bernal environment		0 3 6	9	–	4.666...
Frank–Kasper phases	Various	0 0 12 0	12	–	5.0–
		0 0 12 2	14		5.1111...
		0 0 12 3	15		
		0 0 12 0	16		
Frank–Kasper phase, Cr_3Si	Cr	0 0 12 2	14	–	5.1111...
	Si	0 0 12 0	12		

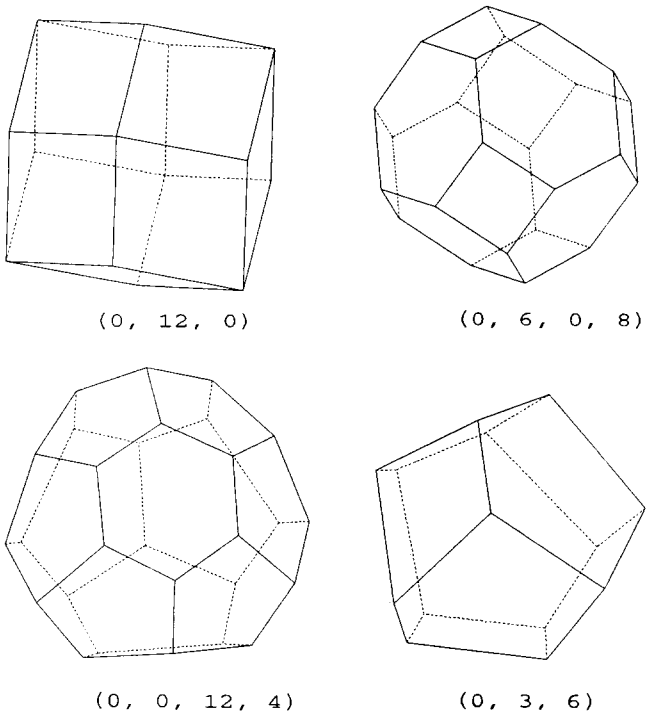

Fig. 1. The Voronoi polyhedra for several basic crystal structures: f.c.c. (0, 12, 0); b.c.c. (0, 6, 0, 8); one of the Frank–Kasper sites (0, 0, 12, 4); a Bernal cell (0, 3, 6).

Frank and Kasper have labelled these lines as major ligand lines (later called $-72°$ disclinations by Nelson [3]).

The Frank–Kasper phases provide a means to relax the frustration inherent in tetrahedral packing. Consider four equivalent atoms, two on a bond line and two common nearest neighbors lying adjacent to the line. The four, attached together, will form a regular tetrahedron. Adding more like-sized common nearest neighbors to the bond line will add more regular tetrahedra sharing a common edge with the first. Now, one can pack

$$q_{\text{tet}} = 2\pi/\cos^{-1}(1/3) = 5.104\ldots$$

regular tetrahedra having a common edge. With q_{tet} being a non-integral number, geometric considerations frustrate tetrahedral packing along a bond line. As Nelson [3] observed, the Frank–Kasper phases accommodate this with their sparse numbers of six-edged facets, leading to structures whose count $\langle q \rangle$ of the average number of common nearest neighbors to a bond line, closely approximates q_{tet}. The chemically important six-edged major-ligand bond lines may form nets extending through the crystal.

To illustrate one application [4] of the construction of major ligand lines, consider the Cr_3Si (A15) phase listed in Table 1. In the form of Nb_3Sn and related compounds, the A15 phases included the highest T_c superconductors prior to the discovery of Bednorz and Müller. The major-ligand lines passing through the (0, 0, 12, 1) Cr sites are the linear transition-metal chains which extend in the x, y and z directions in this structure, and which are also recognized to be important to the chemical bonding of A15 compounds. Application [5] of the Voronoi construction to the copper-oxide high-temperature superconductors is given elsewhere.

Further applications of Voronoi polyhedra and major ligand lines are discussed in Sections 2–5.

The Voronoi construction illustrates how structures affect properties. Another method of comparison, which is in effect the reverse, *i.e.* chemical bonding affecting structure, involves the construction of structural maps. Hume-Rothery noted that parameters such as band filling, electron-to-atom ratio, atomic size, and the like influence the structure that the system will occur in. We will briefly illustrate an example of the importance of size in structural maps in Section 6.

2. αMn:major ligands and supersymmetry

The element manganese displays more complicated structures than the other transition metals. Its room temperature form, αMn, is complex b.c.c., with 58 atoms per unit cell. There are 29 atoms each associated with the (0, 0, 0) and $(\frac{1}{2}, \frac{1}{2}, \frac{1}{2})$ sites. Frank and Kasper [2] originally considered αMn to be a member of the topologically close-packed structures that include the σ, A15, and Laves systems among others, but it has been shown [6] that it does not meet the strict definition. A Voronoi construction shows that the two Mn1 sites are (0, 0, 12, 4), the eight Mn2 sites (0, 0, 12, 4), the 24 Mn3 sites (0, 1, 10, 3), and the 24 Mn4 sites (0, 0, 12, 0). Although the Mn3 site is 14-fold coordinated, its (0, 1, 10, 3) environment does not conform to the Frank–Kasper definition of (0, 0, 12, 2) as the 14-fold coordinated site.

Figure 2 shows the structure of αMn as determined by Bradley and Thewlis [7], where "The basis of the whole arrangement is one single body-centered cubic lattice, but each lattice point is represented by a cluster of 29 atoms." It is instructive to quote further from ref. 2: "These clusters of atoms are in no way chemical molecules or even groups. An atom is no more related to the other atoms within the cluster than to neighboring atoms outside the cluster. The cluster is in fact a mere geometrical conception, serving as an aid to the imagination."

In fact, the cluster of atoms shown in Fig. 2 is not the only possible cluster which will satisfy all the symmetry requirements. However, by constructing major ligand lines appropriate to the crystal structure [8], it is feasible to select from the possible clusters one particular cluster which appears to have a significant

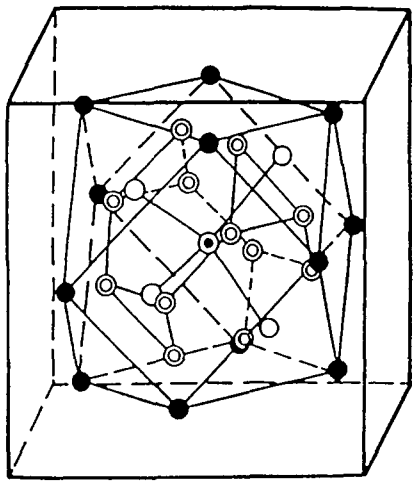

Fig. 2. The structure of αMn as determined by Bradley and Thewlis [7].

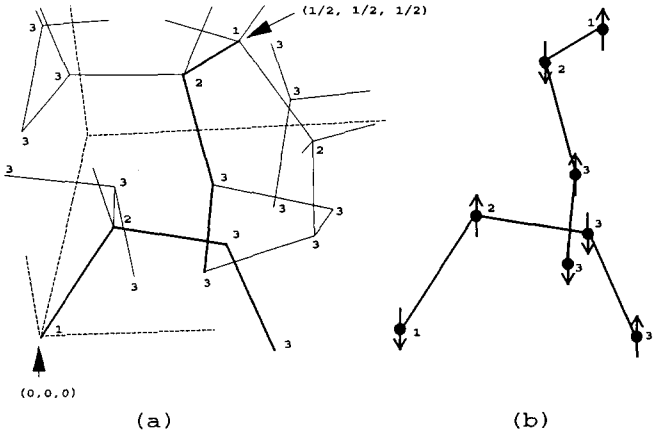

Fig. 3. (a) A sketch of the two networks of major ligands obtained as described in the text. The cartesian axes are shown by dashed lines. The major ligands are indicated by solid lines. Some of these solid lines have been darkened to guide the eye. The atom at the origin and at the body center (labelled 1 for Mn1) are marked by arrows. The Mn1 and Mn2 sites are (0, 0, 12, 4) and hence have four major ligand lines emanating from them. The Mn3 sites are (0, 1, 10, 3) and hence have three major ligand lines. The Mn4 sites are (0, 0, 12, 0) and are not shown here. (b) The same darkened ligand lines are reproduced from Fig. 3(a). In addition, arrows show the orientation of the magnet moments, as described in section 3.

chemical relationship within the cluster. As is evident in Fig. 3(a), there are two independent nets of major ligands extending to infinity in all directions. These nets define the particular cluster of near neighbors around the atom at (0, 0, 0) or ($\frac{1}{2}$, $\frac{1}{2}$, $\frac{1}{2}$) except, of course, for the Mn4 atom which has no six-fold facets. The two nets are identical to each other, except that the cluster defining them is centered at the two defining atoms. (Since the six-fold faces generally involve the nearest of the near neighbors, it is interesting to note that the cluster chosen by these two nets of major ligands is not the same as that illustrated in Fig. 2).

The ring of six common nearest neighbors constituting a six-fold face is forced radially outwards, thus allowing the two atoms connected by a major ligand to pull closer together. Strong chemical bonding (hence the name major ligand) is exhibited by the short bond length as well as by the sharing of the larger than usual number of common nearest neighbors. Also associated with the networks shown in Fig. 3(a) are magnetic effects, a discussion of which is deferred to the next section.

The choice of a unique cluster obtained by the Voronoi construction outlined here, is not consistent with the ordinary rules of crystallography expressed by Bradley and Thewlis. Of course, a unique cluster could be chosen by invoking chemical or other physical arguments, but the unique cluster we have illustrated was determined entirely by geometrical arguments, without chemistry, thermodynamics, or quantum mechanics. The explanation is that the symmetry implicit in the three-dimensional space group approach to crystallography is incomplete, and a supersymmetry, related to projections from higher-dimensional space, is sometimes derivable from the three-dimensional geometry alone. Nelson's [3] view that the Frank–Kasper major ligand lines could be viewed as $-72°$ disclinations arose from a projection from higher-dimensional space.

3. Magnetism

The strength of the magnetic coupling at an atomic site depends on the nature and arrangement of its neighbors. The magnetic coupling at the transition-metal sites and the magnetic moments which reside there can be associated with [9, 10] the Voronoi polyhedra and the major ligands. For example, consider αMn, discussed in the last section, which is an antiferromagnetic material. The magnetic moments at the four sites are shown in Table 2. It is evident that the sites with the largest number of six-sided facets have the most substantial magnetic moments, whereas the site Mn4, with no six-fold facet, has a vanishingly small moment.

The arrangement of the magnetic moments leading to the antiferromagnetism is illustrated in Fig. 3(b). This figure shows some of the atoms in the same positions

TABLE 2. Magnetic moments in αMn

Atom	Point set	Voronoi polyhedron	Magnetic moment
Mn1	2a	(0, 0, 12, 4)	1.9
Mn2	8c	(0, 0, 12, 4)	1.65
Mn3	24g	(0, 1, 10, 3)	0.6
Mn4	24g	(0, 0, 12, 0)	0.2

as in Fig. 3(a), but with the orientation of the magnetic moments at the sites shown. (We ignore the slight spin canting which is found, and consider only parallel and antiparallel orientations. We also ignore the small moment at Mn4.) First, set the spins on the **2a** sites, (0, 0, 0) and $(\frac{1}{2}, \frac{1}{2}, \frac{1}{2})$, as antiparallel, as is usual in antiferromagnetism in b.c.c. crystals. Second, follow along in each network with antiferromagnetic coupling, as shown. This can lead to parallel spins near each other, as can be seen with two Mn3 atoms in the different nets. This simple procedure is in agreement with the assignment of spin directions obtained in neutron diffraction experiments.

Factors such as intersite coupling (implicit in the topology of Voronoi polyhedra) and site volume are both relevant to the local magnetism. Voronoi cell construction can be employed to derive a measure of the local site volumes, and explore their correlations with the magnetic moments [11]. If we assume that all the Mn atoms in αMn have the same radius, then the Voronoi cells have different volumes! Relating these volumes to the magnetic moments at the four Mn sites in α-Mn, a nearly linear relation is found (Fig. 4). Finding an increasing magnetic moment with increasing volume is consistent with the customary experience with the Invar effect.

A similar, although less striking result, is obtained for the four Fe sites in the hard magnet Nd_2Fe_{17}, as is apparent in Fig. 4. Again, the largest magnetic moment is found at the site with the largest number, 2, of major ligands. (Although the (0, 1, 10, 2) also has two major ligands, it is weakened by the presence of one four-fold site, termed a minor ligand by Frank and Kasper.) Again, the volumes calculated from Voronoi cell constructions are correlated with the magnetic moments.

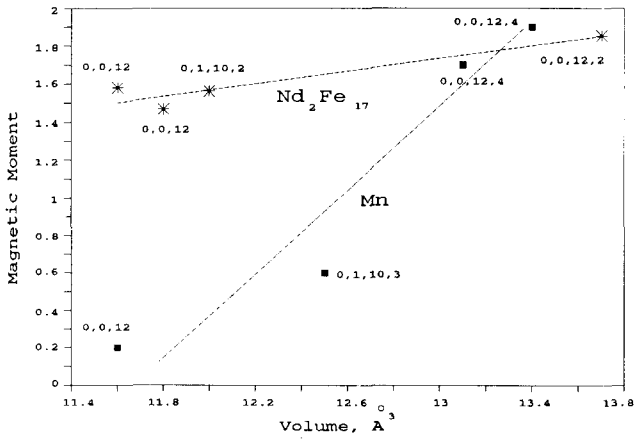

Fig. 4. The magnetic moment, as determined by neutron diffraction, at the four Fe sites in Nd_2Fe_{17}, and at the four Mn sites in αMn, *vs.* the volumes of the Voronoi polyhedra associated with the sites.

Another application of the Voronoi construction to magnetism is in the inspection of magnetic anisotropy. The crystal field anisotropy at a rare-earth site makes an essential contribution to the quality of the hard magnets. The crystal fields depend on the arrangements of the near neighbors of the rare earth. The orientation of the major ligand lines are one way to define [5] the crystal field axes at the rare-earth sites, as illustrated in Table 3. The experimentally observed easy axis of magnetization is shown in the table for the six compounds above the dashed line and these are compared with the orientations of the major ligand nets. Where there are two sets of ligands in two directions, we call the nets that include rare earth–rare earth bonding as principal. Where the bonding is only rare earth–transition metal, the nets are secondary and are shown in brackets in the table. The four compounds below the dashed lines constitute predictions obtained from the Voronoi constructions where there has not been any measurements reported as yet.

Sometimes, the correlations discussed above between major ligand lines and magnetic moments can be used to aid in the unravelling of complicated site occupancy problems. An example is given [13] for RFe_nAl_{12-n} compounds.

4. Polymorphism in metallic glasses

Metallic alloy glasses of transition metal–metalloids, characterized by strong chemical bonding between the transition metal atoms and the metalloids, are easily produced by a variety of methods, including electrodeposition or liquid quenching. These glasses are generally stable at room temperature in the compositional range near deep eutectics in the equilibrium phase

TABLE 3. Observed easy axis of magnetization and orientation of major ligand nets for some prolate rare earth–transition metal compounds

Compound	Observed easy axis	Major ligand nets		
		c-axis	Basal plane	(111)
$Sm_2Fe_{14}B$	*ab* plane	(–R–M–)	R–R clusters	
$SmCo_5$	*c* axis	–R–R–	(–R–M–)	
Tm_2Fe_{17}	*c* axis	–R–R–	(–R–M–)	
Nd_2Fe_{17}	*c* axis	–R–R–M–M–	(–R–M–)	
$ErFe_2$	(111)			–R–R–
$ErNi_3$, Er1	*c* axis	–R–R–R–	(–R–M–)	
Er2	*ab* plane		–R–R–	
$NdMn_{12}$			–R–M–	
$CeMn_6Ni_5$			–R–M–	
$NdCo_9Si_2$		–R–M–		
$CeMnNi_4$				–R–M–

diagram of the alloy system. The eutectic at 19 at.% P for the Ni–P system, as shown in the phase diagram, Fig. 5, is an example.

The metallic alloy glass structure has generally been considered to possess a local symmetry similar to that of an appropriate crystalline counterpart. Since the density of the glasses is universally only a few per cent less than the value for the crystalline material (see *e.g.* Fig. 6), it would not be unexpected to find similar short-range packing of the atoms and similar near neighbor interactions in the glassy state and in the crystalline solid. For those systems in which many stable and metastable crystalline polymorphs are known to exist, it is not clear which form of short-range order will be

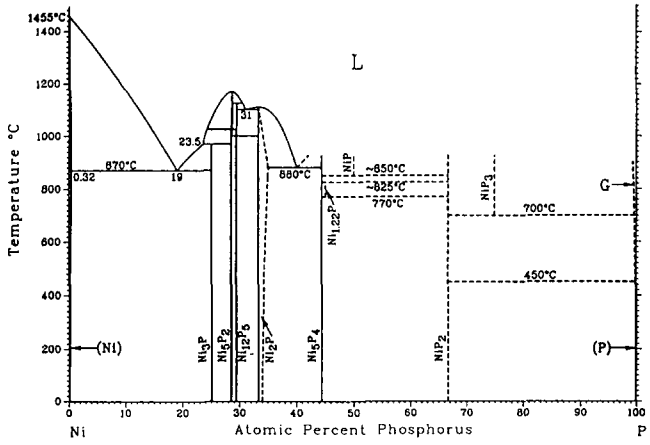

Fig. 5. The Ni–P phase diagram.

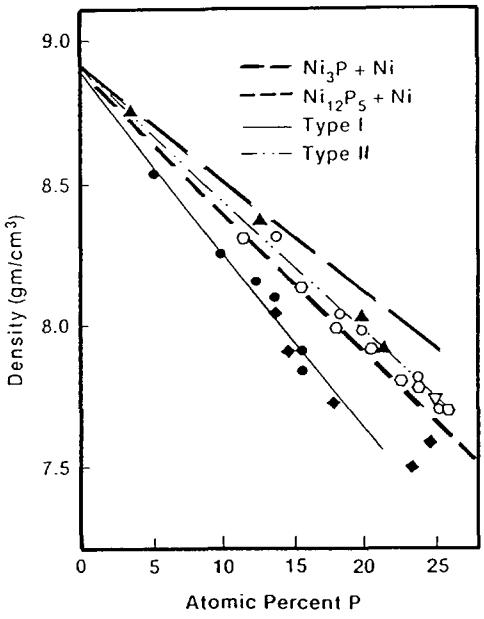

Fig. 6. The density *vs.* composition of Ni–P glassy alloys prepared by different methods. The two thick dashed lines show a theoretical density of a mixture of elemental Ni and the crystalline compound noted. The lines labelled Type I and Type II are to guide the eye through two sets of experimental density data on the glasses.

preferred in the glass, or if the glass will be a mixture of two or more forms of order. There is some experimental evidence for more than one glass-like state dispersed locally in a specimen. Walter *et al.* [14] found that there were two distinct glassy states in melt-spun ribbons of Fe–B alloy. Their interpretation of this result is that there were clusters of differing compositions in the ribbons. This can be likened to the presence of two liquids of differing compositions in a liquid miscibility gap.

In contrast, the glassy analog of polymorphism in Ni–P glasses prepared by different methods has been found [15–17]. The Ni–P metallic glass alloy system has a long history, having been the first [18] material in which the special metallic glass state was observed to exist. Ni–P glasses have been prepared by a wide variety of techniques, including chemical deposition, electrodeposition, and splat quenching. This fact also serves as an indication of its ease of preparation and its relative stability. Finally, as a binary system, Ni–P offers a simplification in the interpretation of experimental results that may be masked in ternary, or higher systems.

Polymorphism differs from phase separation in that the two (or more) structurally distinct phases occur at the same composition, and usually only one of these is prevalent in a sample at a time. Furthermore, a phase transformation between polymorphs differs from structural relaxation in that the latter is a continuous process which occurs during low temperature annealing, whereas the former is an abrupt structural transformation between two distinct phases. Some of these concepts are illustrated in Fig. 6 which shows the density of Ni–P glasses prepared by a variety of processes. It is evident that the measured densities of the Ni–P glasses fall only a few per cent below the density of the corresponding theoretical mixtures of crystals, and thus correspond to two different glass structures. The variations in densities about some mean value correspond to experimental error in the density measurement and to structural relaxation of the glass. These variations are significantly smaller than the difference between the two glasses.

Nuclear magnetic resonance (NMR) Knight shifts, which sample the local electronic structure through the hyperfine interaction, are a very sensitive measure of local environment differences among structures. Knight shift measurements (shown in Fig. 7) on Ni–P glassy alloys [15] have established that there are at least two distinct glassy structures, corresponding to the two sets of densities in Fig. 6. For compositions between approximately 14 and 25 at.% P, a constant Knight shift of approximately 0.16% was measured for d.c. electroplated samples. Over a similar composition range samples prepared by chemical deposition, splat quench-

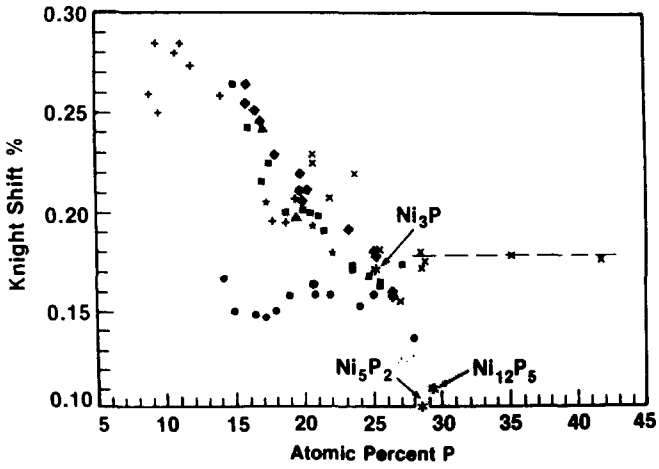

Fig. 7. The nuclear magnetic resonance Knight shifts *vs.* composition for Ni–P glassy alloys prepared by different methods, and for three crystalline compounds. Two distinct bands of data are evident.

ing, and other methods showed a decreasing Knight shift (about 0.28% to 0.15%) with increasing phosphorus concentration. Of particular significance is the bimodal nature of the results; *i.e.*, as Fig. 7 shows, no Knight shifts were recorded in the region between the two sets of data. The absence of data in this region is in contrast to what would be expected if these materials were not structurally distinct, but were related by a relaxation process. Annealing experiments were used to help categorize the lower energy glass.

The density and NMR results lead to an identification of the two glass structures as similar to the two crystalline phases Ni_3P and $Ni_{12}P_5$. Since these crystalline phases can be related to each other through the Landau rules by a second-order phase transition, and if the two glass structures bear a similarity to these, it is possible that the two types of glass transform similarly. Then an average density or Knight shift would not be expected to smear out the bimodal distributions observed. An extended X-ray absorption fine structure (EXAFS) experiment [16] was used to distinguish the character of the local environment for the glasses, in agreement with the identification above of the two glass structures as similar to the two crystalline phases Ni_3P and $Ni_{12}P_5$, and also demonstrated that the two glasses are not related through structural relaxation.

The crystalline phases Ni_3P and $Ni_{12}P_5$ display markedly different metalloid environments. There is one phosphorus site in Ni_3P; its Voronoi polyhedron, (0, 3, 6), is the Bernal cell postulated in the theory of liquids shown in Fig. 1. There are two distinct phosphorus sites in $Ni_{12}P_5$. Over a reasonable range of ratios of P to Ni radii (and for reasonable P site volumes), the Voronoi cells for these two P sites are (8, 0, 0) and (0, 6, 4). These two polyhedra are pictured in Fig. 8. In contrast with the cells of Fig. 1, these

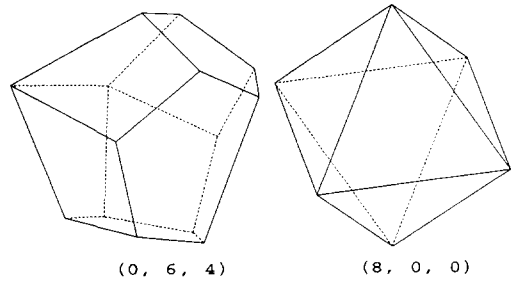

Fig. 8. The Voronoi cells associated with the two phosphorus sites in the crystalline $Ni_{12}P_5$ compound. Note that there are vertices with four lines emanating from them.

two are non-triangulated, in the sense that four (rather than three) planes intersect at a vertex, so that cutting that vertex does not yield a triangle. Such non-triangulated behavior is commonly associated with having four nearest neighbors in a common plane.

The less stable Ni–P glass is seen to be associated with the non-triangulated environment. It is reasonable to presume that non-triangulated environments which arise from an arrangement of four (or more) coplanar neighbors are inherently of higher energy, since the breaking up of the planar arrangement, with its associated four-fold vertex, into two three-fold vertices should probably release energy. Therefore, it might be expected that, if a glass involves non-triangulated metalloid environments, there may be another more stable glassy phase accessible to observation, and some predictions along this line of reasoning have been presented elsewhere [19].

5. Icosahedral phases

Do icosahedral phases ("quasicrystals") have sites with local icosahedral symmetry? To answer that question, the atomic positions of the icosahedral phase must be known, and generally, the structural information now available is too sketchy for this. In the meantime, it is of interest to compare [20] the Voronoi polyhedra, as a measure of the local environment, of the Mn in all the known crystalline phases of Al–Mn with two independent descriptions [21, 22] of the Al–Mn quasicrystalline icosahedral phase for which all the atomic positions are available.

The Al–Mn alloy system has a wide variety of local Mn environments in its many crystal structures. The Mn-site Voronoi polyhedra found in the crystalline Al–Mn systems are shown in Table 4. Many of the Mn sites display the icosahedral (0, 0, 12) polyhedra. The $\mu MnAl_4$ phase has nine distinct sites having the (0, 0, 12) polyhedron. However, none of the crystalline systems in this table are Frank–Kasper phases, where *all* the sites are (0, 0, 12, 0), (0, 0, 12, 2), (0, 0, 12, 3), or

TABLE 4. Voronoi polyhedra appropriate to the Mn sites in the crystalline Mn–Al systems and the principal Mn polyhedra obtained for the icosahedral descriptions; the average Mn site coordination number n is indicated

Crystalline		
$MnAl_{12}$	(0, 0, 12)	$n=12$
$MnAl_6$	(0, 6, 4)	$n=10$
$\mu MnAl_4$	(0, 12), (0, 0, 12) 9 sites	$n=12$
Mn_4Al_{19}	(0, 0, 12), (0, 2, 8, 1)	$n=11.5$
α(Mn–Al–Si)	(0, 0, 12), (0, 2, 8, 1)	$n=11.5$
Mn_3Al_{10}	(0, 0, 12)	$n=12$
β(Mn–Al–Si)	(0, 0, 12)	$n=12$
Mn_4Al_{11}	(0, 2, 8, 2), (0, 3, 6, 4)	$n=12.5$
$Mn_{12}Si_{43}Al_{45}$	(0, 2, 8)	$n=10$
$Mn_3Zn_2Al_{11}$	(0, 2, 8, 1), (0, 3, 6), (0, 0, 12), (0, 8, 2, 2)	$n=11.4$
Icosahedral descriptions		
MDW	(0,3,6,4), (0,3,6,3)+(0,5,6,2), (0,2,8,4)	$n\approx 12.5$
SO	(0,3,6,3), (0,4,6,2), (0,5,6,1), (0,4,4,3)	$n\approx 12$

(0, 0, 12, 4). The striking distribution in crystalline polyhedra, for Al as well as for Mn sites, indicates that Mn and Al accommodate one another in a variety of ways. This accommodation is also evident in the range of volumes per atom that is seen for these alloys and is a manifestation of flexibility in bonding conditions.

In one of the icosahedral descriptions [22], the atomic sites are attributed to the peaks of a mass density wave (MDW). In the vertex version, the sum is taken to span the six independent q vectors of that model (*i.e.* they are directed to the vertices of an icosahedron). Given the $|q|$ as measured by X-ray diffraction, the set of peaks is cut off so as to avoid an unrealistically high atomic density. The other description [21] is derived directly from electron diffraction data from which the same six independent q vectors were derived. Using traditional methods for the analysis of modulated crystals, a sliding origin (SO) model for the Al–Mn icosahedral phase was generated. This description requires interpenetrating rather than space-filling rhombohedral "tiles", where modulations take place along four non-intersecting ⟨111⟩ directions of cubes. Rules for the occupancy of atomic sites are based on a layering-modulation pattern over a reference skeleton. In both the MDW and SO descriptions, the modulated (aperiodic) atomic motifs fill space – there are no holes or gaps.

Applying the Voronoi constructs, the resulting measures of local environments in the two descriptions are in agreement with one another and with experiment.

(i) There is a distribution of Mn site Voronoi polyhedra topologies (displayed in Table 4) and an even broader one of Al site topologies.

(ii) There is a wide range in site metrics and volumes. The volumes were found to span those appropriate to Mn and Al and they tend to fall into two well defined groups. The MDW description decided which sites are occupied by Mn by the fact that approximately 20% of the sites are characteristic of Mn volumes. In the SO description, the sites occupied by Mn are determined by layering along the modulation directions, and this was found to be consistent with the same volume considerations used in the MDW description.

(iii) No sites were found using the building blocks of the Frank–Kasper structures. (Some (0,0,12) sites were found for a face (as against the vertex) version, in the mass density description.)

(iv) The radial distribution functions (RDF) for the two descriptions show nearest neighbors lying between 0.25 and about 0.3 nm in a bimodal distribution. The SO description's RDF was inspected at larger distances and narrow peaks were observed at about 0.6 nm. This implies long-range positional correlations characteristic of a crystal and inconsistent with a glass. The main difference between the MDW and the SO icosahedral descriptions is the MDW's somewhat higher average coordination number (i.e. the total number of faces of a polyhedra), approximately 12.5 *vs.* approximately 12. The crystalline environments, ranging from 9 to 13, span this range.

The considerations above for the Mn–Al system may not apply to icosahedral phases in other systems. Just as there is more than one way to pack atoms in traditional crystals, there can be more than one icosahedral packing. For example, the Al–Cu–Li system contains a phase (with the *cI*162 structure) that has a Frank–Kasper structure. Perhaps the Al–Cu–Li icosahedral phase has Frank–Kasper packing, and maybe it could be described by the face version of the mass density description.

6. Structural maps

It has been long recognized that simple physical parameters can play a controlling role in phase formation. For example, a binary substitutional alloy is

unlikely to occur over any significant composition range if the two constituents are too unlike in size. Hume-Rothery, and others, pioneered in rationalizing phase formation trends in such simple terms, two of the other parameters being the electron-to-atom ratio (that is the extent to which bands are occupied) and the strength of bonding, which is traditionally measured as a difference in electronegativities. Often, more than one parameter appears to play a role and a structural map can be drawn using these parameters as coordinates. One example of such a map is shown in Fig. 9 for the occurrence and non-occurrence of transition metal–transition metal Laves phases. One map coordinate is a measure of d band filling appropriate to the compound in question and the other a measure of the difference in atomic sizes of the constituents. (The Laves structures show a volume contraction, relative to the sum of the elemental metal atomic volumes, and this construction has been assigned to the electropositive minority A atom when plotting the elemented volume ratios.) The map is remarkable in having its boundaries parallel to its coordinates. (The upper boundary depends on the data for Mn_2La alone.) Aside from the overall success of the map in accounting for Laves phase formation, what is of interest are the "errors" in the plot. Rh_2Sc is the system whose position is most deeply embedded in the Laves region, for which neither a Laves structure nor any other 2:1 phase has been reported. The Rh–Sc system has not been completely investigated and the mark suggests that further investigation will yield a Laves phase. There are several vanadium compounds (V_2Zr, V_2Hf, V_2Ta) which do form Laves phases and which lie outside the Laves region to its right. It remains to be seen whether these phases have been stabilized by defects or impurities or whether they represent true errors in the map.

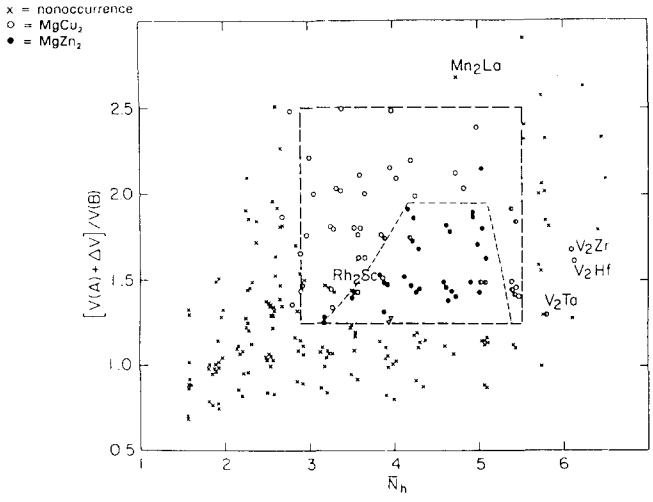

Fig. 9. A structural map for the occurrence and non-occurrence of transition metal–transition metal Laves phases. An × indicates a binary pair for which a Laves structure has not been recorded either because it does not occur or because it has yet to be observed.

Structural maps have been employed by Villars, Pettifor, Phillips and Rabe elsewhere in this meeting. These maps have had considerable success employing different sets of coordinates.

7. Summary

In this paper, we have described how the purely geometric construction of Voronoi polyhedra, modified to account for differing atomic radii, provides valuable insight in discussions of a variety of interesting phenomena in crystallography, magnetism, and metallic glasses, and icosahedral phases. Although this insight might be "obvious" in simpler crystal structures, such as the chains of atoms important to superconductivity in the A15 structures, the insight may be "startling" in more complex structures, such as in the discovery of supersymmetry in αMn. Specific predictions are presented to be checked by future experiments, including the occurrence or non-occurrence of metastable glassy phases in transition-metal–metalloid glasses, and the orientation of the crystal field axes at the rare-earth sites in magnetic materials.

Acknowledgment

R.E.W. at Brookhaven National Laboratory is supported by the Division of Materials Science, USDoE, under contract DE-ACO2-76H0016.

References

1 W. Fischer, E. Koch and E. Hellner, *Neues Jahrb. Mineral. Monatsh.*, (1971) 227.
B. J. Gelattly and J. L. Finney, *J. Non-Cryst. Solids, 50* (1982) 313.
2 F. C. Frank and J. S. Kasper, *11* (1958) 184; *12* (1959) 483.
3 D. R. Nelson, *Phys. Rev. B, 28* (1983) 5515.
4 L. H. Bennett, R. E. Watson and W. B. Pearson, *J. Magn. Magn. Mater., 54–57* (1986) 1537.
5 M. Melamud, L. H. Bennett and R. E. Watson, *Phys. Rev. B, 38* (1988) 4624.
6 R. E. Watson and L. H. Bennett, *Scr. Metall., 19* (1985) 535.
7 A. J. Bradley and J. Thewlis, *Proc. R. Soc. London, 115* (1927) 456.
8 L. H. Bennett and R. E. Watson, *Phys. Rev. B, 35* (1987) 845.
9 R. E. Watson, M. Melamud and L. H. Bennett, *J. Appl. Phys., 61* (1987) 3580.
10 R. E. Watson, L. H. Bennett and M. Melamud, *J. Appl. Phys., 63* (1988) 3136.

11 L. H. Bennett, R. E. Watson and M. Melamud, *J. Phys., (Paris) 49* (1988) C8-537.
12 M. Melamud, L. H. Bennett and R. E. Watson, *Scr. Metall., 21* (1987) 573.
13 M. Melamud, L. H. Bennett and R. E. Watson, *J. Appl. Phys., 61* (1987) 4246.
14 J. L. Walter, S. F. Bartram and I. Miller, *Mater. Sci. Eng., 36* (1978) 193.
15 L. H. Bennett, H. E. Schone and P. Gustafson, *Phys. Rev. B, 18* (1978) 2027.
D. S. Lashmore, L. H. Bennett, H. E. Schone, P. Gustafson and R. E. Watson, *Phys. Rev. Lett., 48* (1982) 1760.
16 L. H. Bennett, G. C. Long, M. Kuriyama and A. I. Goldman, in G. E. Walrafen and A. G. Revesz (eds.), *Structure and Bonding in Noncrystalline Solids,* Plenum, New York, 1986, p. 385.
A. I. Goldman, G. G. Long, L. H. Bennett, D. S. Lashmore and M. Kuriyama, *J. Electrochem. Soc., 135* (1988) 1919.
17 R. E. Watson and L. H. Bennett, *J. Magn. Magn. Mater., 54–57* (1986) 295.
18 A. Brenner and G. E. Riddel, *J. Res. NBS, 37* (1946) 31; *39* (1947) 385.
19 R. E. Watson and L. H. Bennett, *Phys. Rev. B, 43* (1991) 11642.
20 L. H. Bennett, M. Kuriyama, G. G. Long, M. Melamud, R. E. Watson and M. Weinert, *Phys. Rev. B, 34* (1986) 8270.
21 M. Kuriyama and G. G. Long, *Acta Crystallogr., A, 42* (1986) 164.
22 R. E. Watson and M. Weinert, *Mater. Sci. Eng., 79* (1986) 105.